JTTEE5 16:991–997
DOI: 10.1007/s11666-007-9125-5
1059-9630/$19.00 © ASM International

Microstructure Control of Thermally Sprayed Co-Based Self-Fluxing Alloy Coatings by Diffusion Treatment

Kazunori Sakata, Kosuke Nakano, Hirofumi Miyahara, Yasuhiro Matsubara, and Keisaku Ogi

(Submitted March 29, 2007; in revised form September 8, 2007)

This article describes microstructure control aimed for wear-resistance improvement of Co-based (Co-Cr-W-B-Si) self-fluxing alloy coating by diffusion treatment. The diffusion treatments of thermally sprayed Co-based self-fluxing alloy coating on steel substrate were carried out at 1370-1450 K for 600-6000 s under an Ar gas atmosphere. Microstructural variations of the coating and the interface between the substrate and the coating were investigated in detail. A proper diffusion treatment precipitates two kinds of fine compounds in Co-based matrix. X-ray diffractometer (XRD) and electron probe micro-analyzer (EPMA) analysis revealed these precipitates to be a chromium boride dissolving cobalt and a tungsten boride containing cobalt and chromium. The size of each precipitate became larger with increasing treatment temperature and time. A coating with the proper size borides showed a superior wear-resistance.

Keywords cobalt-based self-fluxing alloy, flame spraying, hardness, microstructure, post heat treatment, wear-resistance

1. Introduction

The thermal spraying of a self-fluxing alloy has been widely used when a thicker wear-resistant and corrosion-resistant coating is needed. A self-fluxing alloy is produced by adding a few percentages of boron (B) and silicon (Si) to nickel (Ni)-based or cobalt (Co)-based alloys. Both elements lower the melting point of the alloy. B addition leads to the precipitation of borides in a matrix, which contribute to the increase in the hardness and the wear-resistance. Also, the self-fluxing alloys are resistant to sulfuric acid, hydrochloric acid, and alkali sodium carbonate (Ref 1). A number of studies have been made on the self-fluxing alloy sprayed coating, but most studies are focused on Ni-based self-fluxing alloys (Ref 2-13), a few studies are conducted on Co-based self-fluxing alloys (Ref 14-16) and no report on systematic study of a Co-based self-fluxing alloy sprayed coating is found. Accordingly, in this study, a basic research for the optimization of microstructure by the diffusion treatment has been conducted on thermally sprayed Co-based self-fluxing alloy coatings through the analysis of microstructure and wear-resistance of the as-sprayed and diffusion-treated coatings.

2. Materials and Experimental Procedure

The chemical compositions of Co-based self-fluxing alloy powder (FP-160M: Fukuda Metal Foil & Powder Co. Ltd., Kyoto, Japan) and mild steel substrate (TC10M: Sumitomo Metals Industries, Ltd., Osaka, Japan) used in this experiment are shown in Table 1. The alloy powder was produced by a gas atomization process for the use of commercial flame spraying equipments. Actual particle size distribution was obtained by using two sets of laser diffraction particle size analyzers (MT3300EX, Microtrac Inc., and Granulometer 1064L, CILAS). The mean particle size was 99.9 μm.

As a surface preparation of the steel substrate (100 mm × 200 mm × 4 mm), ultrasonic cleaning was carried out in an ethyl alcohol bath for degreasing, and abrasive blasting was made using 250-750 μm Al_2O_3 grit so that the surface roughness was set to 50-80 μm Rz. Subsequently, about 1 mm thick thermally sprayed coating was formed on the substrate, using a six-axis robot with powder flame spraying equipment (TeroDyn system 3000,Eutectic of Japan). Spray parameters are shown in Table 2.

X-ray diffractometer (XRD) and electron probe microanalyzer (EPMA) were used for phase identification in

This article is an invited paper selected from presentations at the 2007 International Thermal Spray Conference and has been expanded from the original presentation. It is simultaneously published in *Global Coating Solutions, Proceedings of the 2007 International Thermal Spray Conference*, Beijing, China, May 14-16, 2007, Basil R. Marple, Margaret M. Hyland, Yuk-Chiu Lau, Chang-Jiu Li, Rogerio S. Lima, and Ghislain Montavon, Ed., ASM International, Materials Park, OH, 2007.

Kazunori Sakata, Fujikikosan Corporation, Kitakyushu, Japan; **Kosuke Nakano** and **Hirofumi Miyahara**, Kyushu University, Fukuoka, Japan; **Yasuhiro Matsubara**, Kurume National College of Technology, Kurume, Japan; and **Keisaku Ogi**, Oita National College of Technology, Oita, Japan. Contact e-mail: sakata@fjk-kk.co.jp.

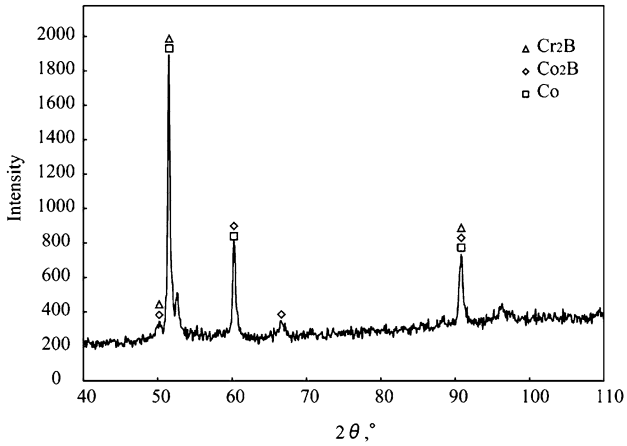

Fig. 1 XRD spectra of the Co-based self-fluxing alloy powder

Table 1 Chemical compositions of powder and substrate

	Chemical compositions, mass%					
Powder	Co	Cr	W	B	Si	Ni
FP-160M	Bal.	21.0	5.09	2.96	1.81	0.69
Substrate	Fe	C	Mn	Si	P	S
TC10M	Bal.	0.08	0.01	0.40	0.013	0.003

Table 2 Spray parameters

Gas	C_2H_2	O_2
Pressure	103.4 kPa	361.9 kPa
Rate of flow	1.5 m^3/h	2.5 m^3/h
Spraying distance	200 mm	
Traverse speed	16 m/min.	
Feed pitch distance	15 mm/pass	

starting powder, as-sprayed and diffusion-treated coatings. XRD was conducted using a Co target at a diffraction angle (2 θ) of 40° to 110°, a scanning step of 0.1°, and a scanning speed of 2°/ min. Identification of the diffraction peak was conducted based on the JCPDS card list.

In EPMA-WDS analysis, the ratio (relative intensity) of the characteristic x-ray intensity from the alloy powders or coated specimens to that from the pure metal was measured, and then the alloy content was determined by the ZAF correction method which evaluated the atomic number effect, the absorption effect and the fluorescence effect on the characteristic x-ray intensity.

In order to clarify the crystallization temperature of the Co-based self-fluxing alloy, the alloy powder (about 30 g) was melted at 1750 K and then cooled at 10 K/min in an electric furnace under an Ar gas atmosphere. Several samples were quenched during solidification, and the freezing sequence of the alloy was identified based on the changes in quenched structure.

Thermally sprayed specimens were cut into square coupons (15 mm × 15 mm) and subjected to diffusion

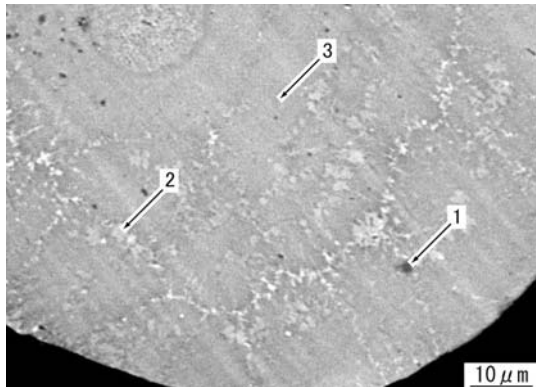

Fig. 2 EPMA compo-image showing the microstructure of the Co-based self-fluxing alloy powder particle

treatment in an electric furnace previously heated at the designated holding temperature under an Ar gas atmosphere. The specimens were heated at a mean speed of 3.25 K/s, kept for 600-6000 s at each holding temperature and then quenched in water. The surface appearance, porosities, and microstructure were examined on each treated specimen.

Vickers hardness and abrasion resistance were examined on the specimen (30 mm × 50 mm). SUGA abrasion tester (NUS-ISO-3, SUGA TEST INSTRUMENT Co. Ltd.) was employed for an abrasive wear test and an abrasive paper with SiC (#320) grit was used as the counterpart. The abrasion test was conducted at a load of 29.4 N, and an abrasion weight loss was measured every 300 double strokes (ds), and this was repeated ten times. New abrasive paper was employed every 300 ds in accordance with JIS H 8682-1 based on the ISO 8351 and ISO 10074.

3. Results and Discussion

3.1 Microstructure of Co-Based Self-Fluxing Alloy Powder

X-ray diffractometer and electron probe microanalyzer analysis were used to investigate the microstructure and constituent phases of Co-based self-fluxing alloy powders. The XRD of the alloy powder revealed the existence of three phases of Cr_2B, Co_2B, and α, as shown in Fig. 1. Further, EPMA compo-image of the particle shows a black region (1), white region (2), and gray region (3), as seen in Fig. 2, however, the structure is too fine to analyze quantitatively.

3.2 Thermal Analysis and Solidification Structure

Figure 3 shows the thermal analysis curve of the Co-based self-fluxing alloy and the structures of specimens quenched during solidification and the crystals identified by EPMA analysis. The microstructure and EPMA analysis of the specimen after solidification are also given in Fig. 4. It is found that (1) and (2) mainly consist of Co, Cr,

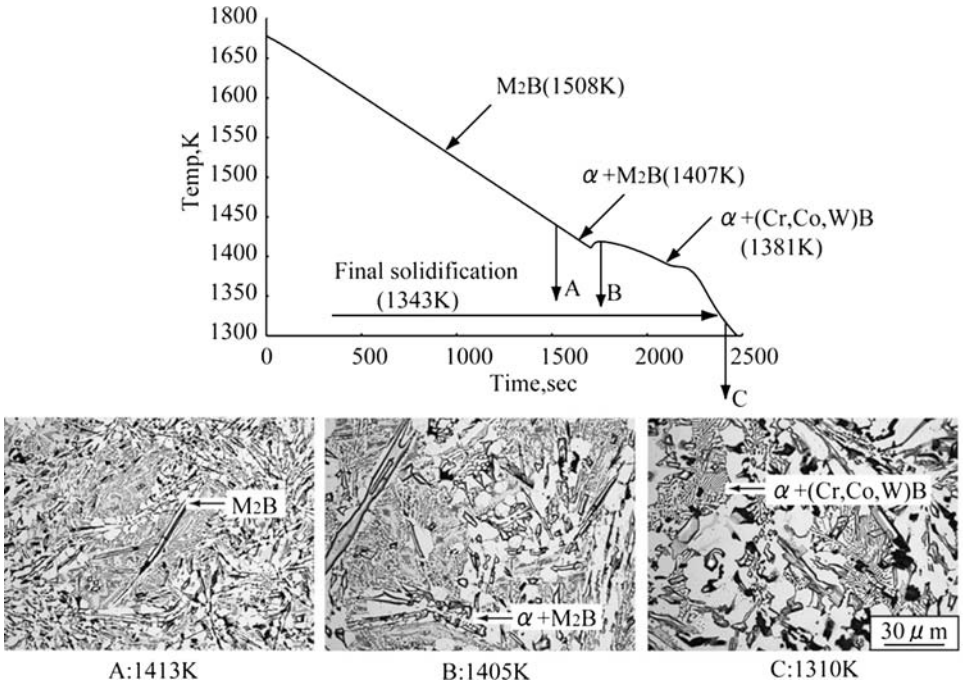

Fig. 3 Thermal analysis curve and solidification structure of Co-based self-fluxing alloy cooled at 10 K/min

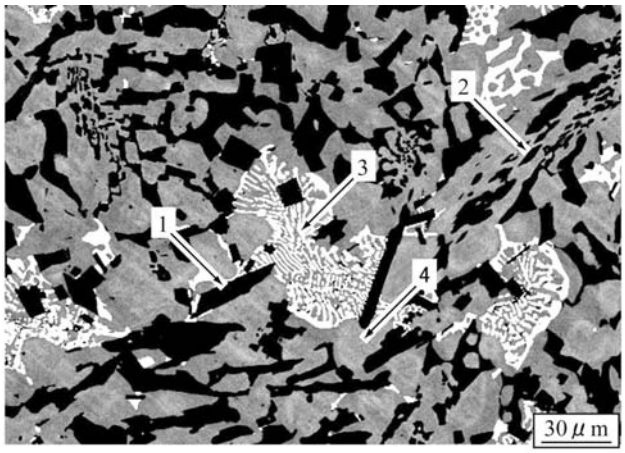

	Co	Cr	W	B	Si	Ni	
1	47.4	42.2	1.88	8.26	0.00	0.20	M_2B(primary)
2	46.3	44.6	1.67	7.19	0.03	0.21	M_2B(eutectic)
3	45.6	17.2	30.6	5.79	0.43	0.42	(Cr,Co,W)B
4	78.3	16.2	2.17	0.00	2.51	0.88	Matrix

Fig. 4 EPMA compo-image and quantitative analysis result (%) of Co-based self-fluxing alloy specimen quenched after solidification

and B, (3) mainly consists of Co, Cr, W, and B, and (4) consists of Co and Cr. These results indicate that primary M_2B (M:transition metals, for example Co,Cr) start to crystallize at 1508 K and grows in rod-like morphology and the eutectic reaction of $\alpha + M_2B$ starts at 1407 K and grows cellularly. Then, $\alpha + (Co, Cr, W) B$ eutectic crystallizes at 1381 K.

Table 3 Variation of surface roughness of coatings with diffusion treatment. (Holding time: 1200 sec.)

Treatment temperature, K	As-sprayed	1378	1392
Surface roughness Ra, μm	24.3	21.9	21.9
Treatment temperature, K	1397	1406	1418
Surface roughness Ra, μm	17.7	17.3	7.17

3.3 Effect of Diffusion Treatment on the Structure of Sprayed Coating

Since the Co-based self-fluxing alloy starts to solidify at 1508 K and the solidification is complete at 1343 K as shown in Fig. 3, the diffusion treatment was conducted in the range of 1378-1418 K, to heat the coating in the solid-liquid coexistence region. The surface roughness (Ra) of the diffusion-treated and as-sprayed coatings are shown in Table 3. The surface of the heat-treated specimen shows a metallic luster and the surface roughness lowers with increasing temperature. However, the specimens treated at 1392 K or lower temperatures show surface roughness slightly lower than that of the as-sprayed specimen. The roughness was substantially lowered by heating at 1418 K.

In order to investigate the effect of the diffusion treatment on the microstructure of the thermally sprayed coating, the cross sections of specimens were observed with an optical microscope, as shown in Fig. 5. Thermally sprayed particles solidified as a solid solution or α phase with very fine precipitates because thermally sprayed particles rapidly solidify on the substrate. Near original

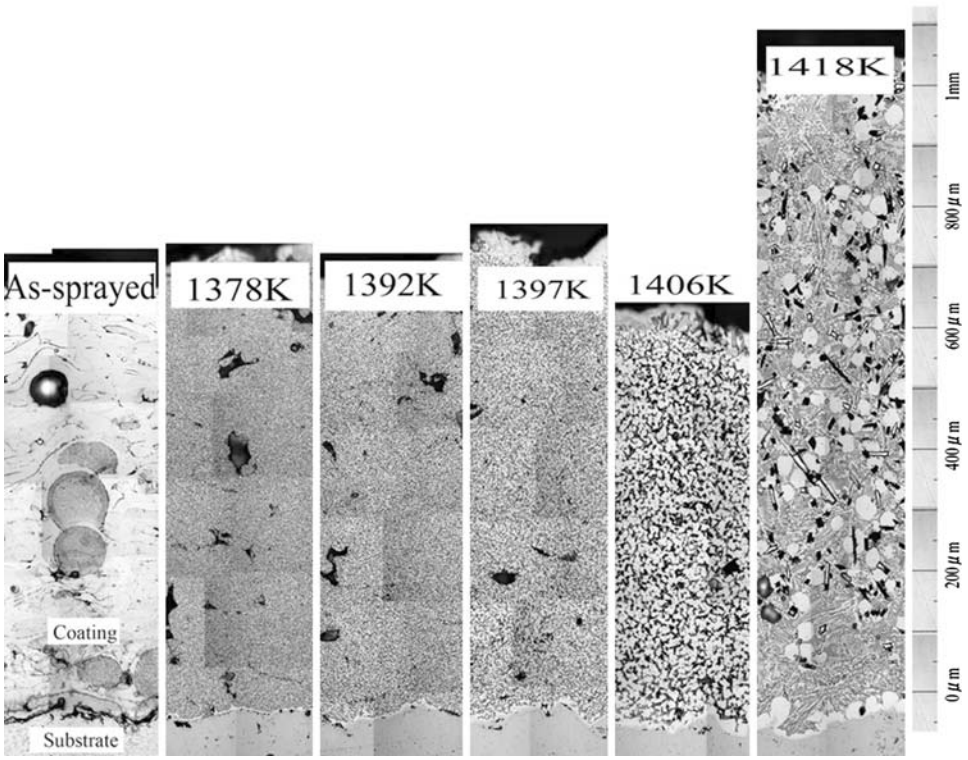

Fig. 5 Optical microscope image of the cross-section of as-sprayed and diffusion-treated coatings (holding time 1200 sec)

spherical particles and significantly flattened particles are observed, and this difference in the shape of particles arises from the difference in thermal energy and kinetic energy given to each particle during thermal spraying. The microstructure of as-sprayed particles is too fine to be observed by optical microscope. For the as-sprayed specimen, extensive cracks were observed at the interface between the substrate and the coating, and porosities exist among particles in the coating. Cracks might be arisen from defects at the interface during preparation of specimen for metallographic examination. In the specimen treated at 1378 K, very fine particles uniformly precipitated in the whole region of the coating. Cracks that appeared at the interface in the as-sprayed specimen mostly disappeared, and precipitate free layer was formed in the interface. Most porosities in the coating also disappeared. The structures of the coatings treated at 1392, 1397, and 1406 K exhibit uniform precipitates in the whole region of the coating and sound interface. With increasing heating temperature, the precipitates become larger, pores in the coating decrease, and the precipitation free layer near the interface becomes slightly wider. Further, the 1418 K treated specimen shows the eutectic structure and rare porosities in the whole region of the coating.

As shown in Fig. 6, the XRD analysis on the surface of the coatings treated at 1378, 1406, and 1418 K reveals that three phases of Co_2B, Cr_2B, and α exist in every coating. The diffraction peaks of the as-sprayed specimen show similar peaks to those of the starting powder and also the existence of a small amount of the amorphous phase. On the other hand, every diffraction peak from the diffusion-treated coating is sharper than that of the as-sprayed specimen.

EPMA compo-image and quantitative analysis of the specimens heated at 1378, 1406, and 1418 K as well as the as-sprayed specimen were made, and as an example, the compo-image near the interface between the coating and the substrate treated at 1406 K is shown in Fig. 7. The microstructure of the coating is composed of a cylindrical black precipitate (1), a fine white precipitate (2), and a gray matrix (3). The coating has no cracks at the interface. The result of quantitative analysis shown in Fig. 7 reveals that these black precipitates consist mainly of Co, Cr, and B, hence black precipitates are identified as M_2B. The white precipitates are consisted mainly of Co, Cr, W, and B, so that they are not identified by the diffraction peaks nor by the phase diagram, so it is assigned to (Co, Cr, W) B. The gray matrix consists mainly of Co and Cr.

The compo-image and quantitative analysis of a coating heated at 1418 K are shown in Fig. 8. The microstructure shows typical four phases. The black cylindrical phase (1) mainly consists of Co, Cr, and B, and is identified as M_2B. The complex regular mixture of white and black phases (2) is revealed to be $\alpha + M_2B$ eutectic. The white phase (3) which is not identified by the diffraction peaks, consists mainly of Co, Cr, W, and B, however, it is assigned as (Co, Cr, W) B. The gray matrix (4) is comprised mainly of Co and Cr. Thus, the coating treated at 1378-1406 K is composed of fine M_2B and (Co, Cr, W) B precipitates dispersed in the α matrix, and therefore the precipitates grow

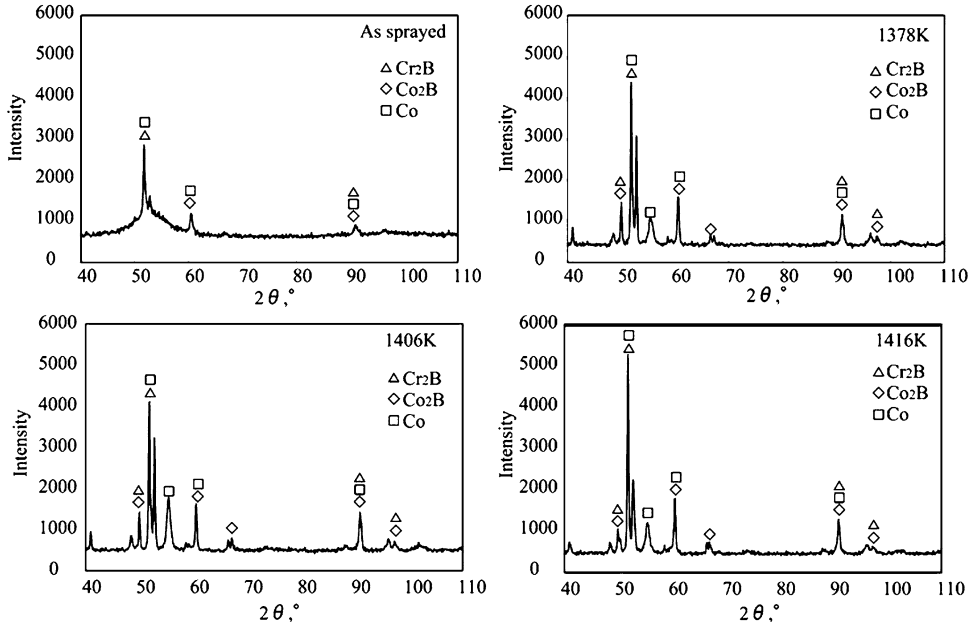

Fig. 6 XRD spectra of the as-sprayed coating and the diffusion-treated coatings (holding time 1200 sec)

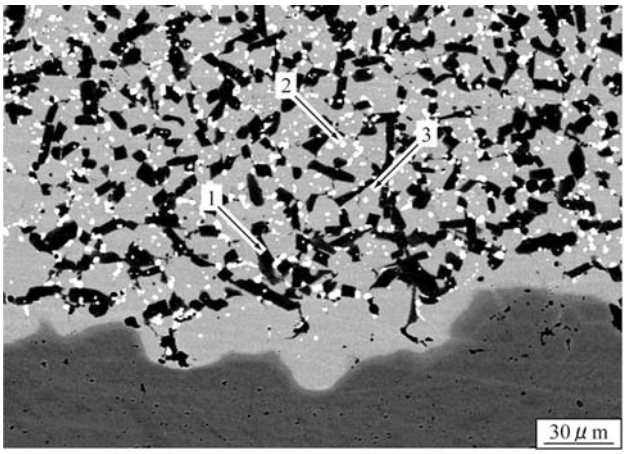

	Co	Cr	W	B	Si	Ni	Fe	
1	46.5	40.4	2.20	8.07	0.01	0.13	2.67	M_2B(primary)
2	36.5	19.0	37.1	6.30	0.00	0.20	0.90	(Cr,Co,W)B
3	77.0	14.8	2.44	0.00	1.88	0.86	3.04	Matrix

Fig. 7 EPMA comp-image of the coating and steel substrate interface in the specimen diffusion-treated at 1406 K (holding time 1200 sec)

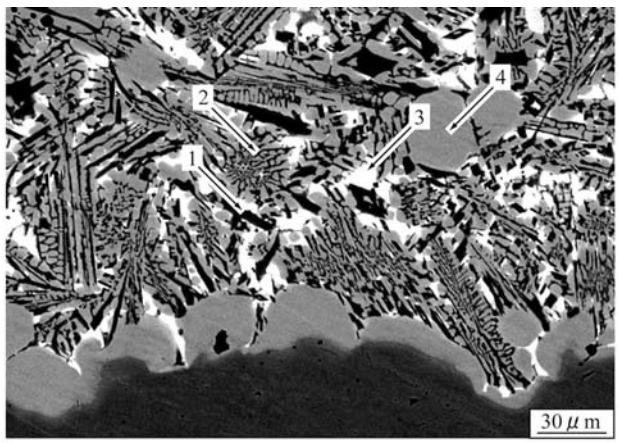

	Co	Cr	B	W	Si	Ni	Fe	
1	54.5	31.8	8.25	3.92	0.00	0.25	1.20	M_2B(primary)
2	66.9	20.7	6.49	3.28	0.54	0.33	1.74	M_2B(eutectic)
3	62.7	12.5	3.37	18.3	1.30	0.64	1.09	(Cr,Co,W)B
4	76.8	16.4	0.00	2.57	1.80	0.79	1.68	Matrix

Fig. 8 EPMA compo-image near the interface of the coating and the steel substrate in the specimen heat-treated at 1418 K (holding time 1200 sec)

with an increase in treatment temperature. When the temperature is raised to 1418 K, the coating melts and solidifies to form primary M_2B, $\alpha + M_2B$ eutectic and (Co, Cr, W) B during cooling.

As indicated in Fig. 7 and 8, a thin layer of precipitate-free α phase is distributed along the interface between the coating and the substrate. To reveal the formation process of this layer, EPMA line analysis was conducted across the interface as shown Fig. 9. The line analysis shows that Co, Cr, W, Ni, and Si diffuse from the sprayed coating layer to the substrate, and Fe and Mn from the substrate to the coating. A similar diffusion pattern of elements is observed in each specimen heated at 1378-1418 K, thus the diffusion treatment allows each element present in the coating and substrate to diffuse and improves the metallurgical bonding at the interface. From these results, it is found that the precipitate free layer formed along the interface is caused by a mutual diffusion of Co, Cr, W, Ni, and Si from the coating, and Fe and Mn from the substrate.

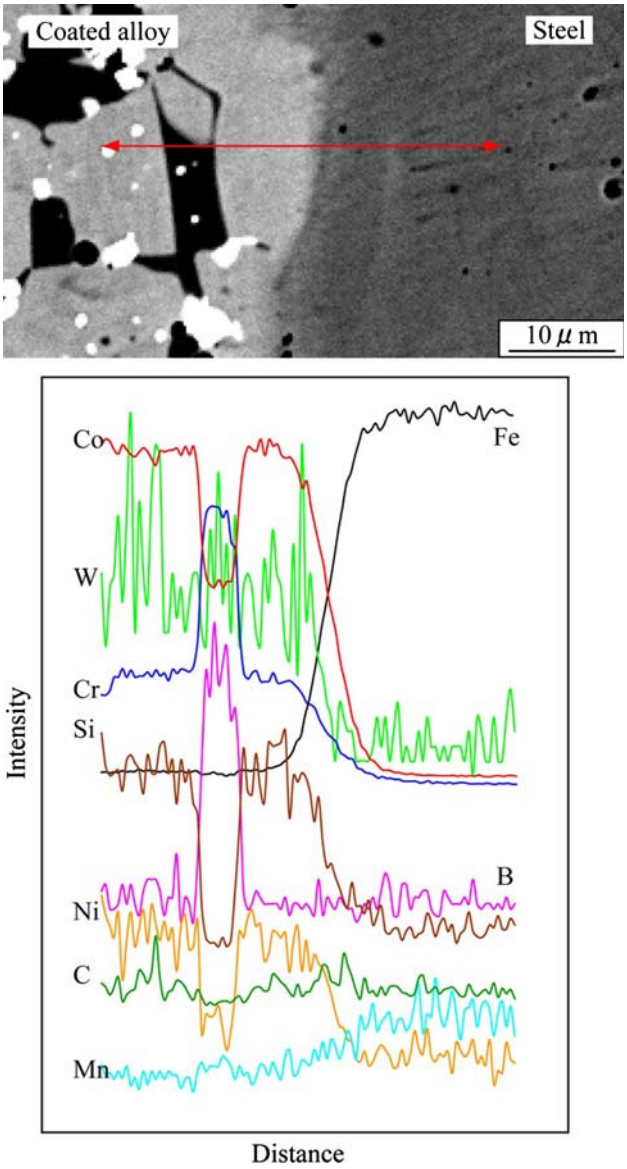

Fig. 9 EPMA line analysis image of across the coating/substrate interface in specimen heat-treated at 1406 K (holding time 1200 sec)

The width of the precipitate free layer increases with the increase in heating temperature and holding time, as shown in Fig. 10. The bonding between the coating and substrate should be strengthened by this mutual diffusion process of elements.

3.4 Effect of the Heat Diffusion Treatment on Hardness and Abrasion Properties

Figure 11 shows the micro-hardness distribution across the coating/substrate interface of the as-sprayed and heat-treated specimens. The heat-treated specimens show higher substrate hardness, because these specimens were quenched after heating at a high temperature. As for the as-sprayed specimen, the hardness of the coating is not

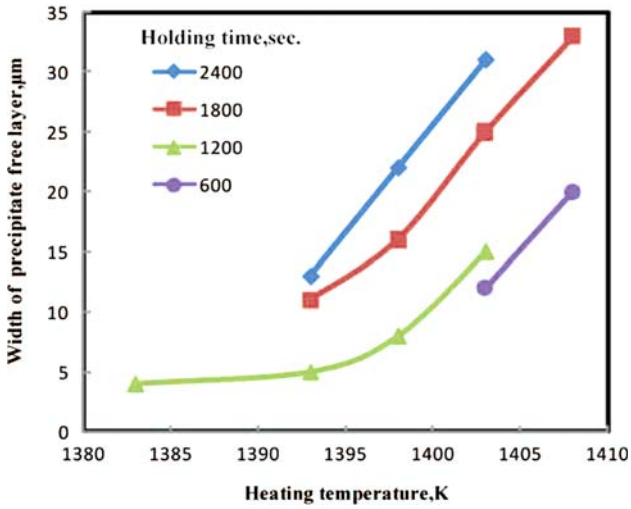

Fig. 10 Effect of heating temperature and holding time on the width of the precipitates free layer

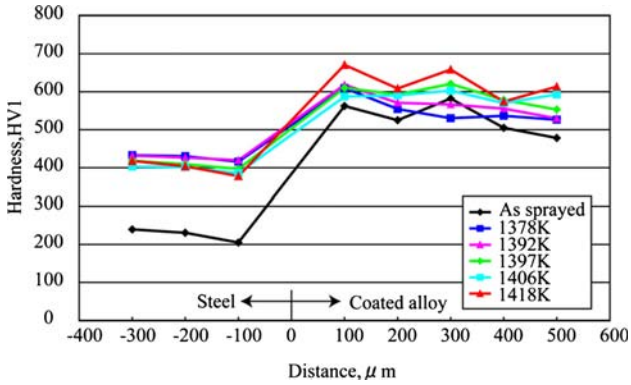

Fig. 11 Coating hardness distribution across the coating/substrate interface

uniform because of porosities. On the other hand, the coatings heat-treated at 1378-1406 K show substantial uniform hardness, because the structure of the coatings consist of α matrix with fine precipitates and less porosities. The coating treated at 1418 K shows some variations in hardness. This is because the diffusion treatment at 1418 K causes a coarse solidification structure composed of hard compounds and a softer α matrix. The hardness level of the coating becomes slightly higher with the increase in heating temperature, this may be caused by the coarseness of the microstructure and the reduced porosity.

The abrasion weight loss of every specimen (see Fig. 12) increase with the abrasion distance, and the specimen heated at 1397 K shows the lowest loss. The specimen heated at 1418 K shows a higher abrasion rate in spite of its higher hardness. The abrasive paper of 320 meshes was used in this experiment, and the diameter of SiC particles on the paper is less than 40 μm. SiC particles should abrade the surface of the specimen with shaper tips. The specimen heated at 1418 K consisted of course solidification structure and size of primary α is about

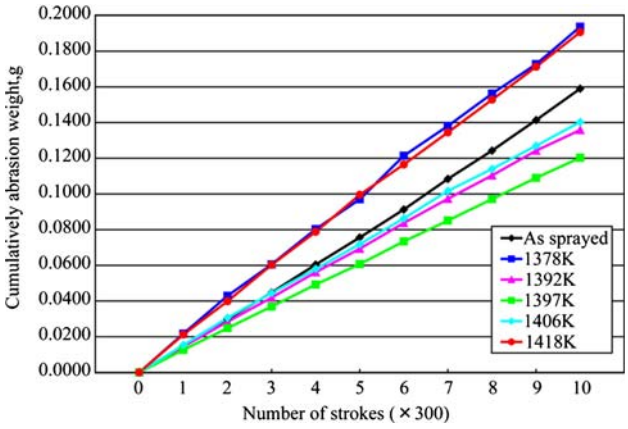

Fig. 12 Abrasion test results of diffusion-treated coatings

30 μm. Therefore, SiC particles might preferentially abrade the Co matrix, then the extruded borides might be broken off. In the specimens heated at 1392 K-1406 K, fine precipitates of 0.9-5.4 μm diameter homogeneously distribute, which should protect Co matrix from the abrasion by SiC particles. When the precipitates are too small, the resistance to abrasion becomes less, the precipitated particles may be abraded together with matrix. It seems the amorphous or supersaturated Co matrix in the as-sprayed coating has rather higher abrasion resistance than the Co matrix with very fine precipitates. The uniform distribution of moderate size of precipitates contributes to higher abrasion resistance.

4. Conclusions

The microstructure control of a Co-based self-fluxing alloy by diffusion treatment has been conducted, and the following results are obtained.

(1) The Co-based self-fluxing alloy powders produced by a gas atomization process consists of Cr_2B, Co_2B, and α.

(2) At the cooling rate of 10 K/min, the Co-based self-fluxing alloy solidifies in the order of primary M_2B at 1508 K, an $\alpha + M_2B$ eutectic at a temperature of 1407 K, and α + (Co, Cr, W)B eutectic at 1381 K.

(3) When the Co-based self-fluxing alloy powders are thermally sprayed on a steel specimen, the flattened particles composed of M_2B, (Co, Cr, W) B, and α build up. M_2B and (Co, Cr, W) B in the thermally sprayed coating are coarsened by diffusion treatment, and the compound becomes larger with increasing temperature. Most of the particles are melted at 1418 K, which solidifies in a coarse structure of M_2B, (Co, Cr, W), B, and α.

(4) A diffusion treatment temperature of 1397-1406 K substantially improves the abrasion resistance.

References

1. M.C. Parsons, Thermal Spray Superhard Coating, *Preprints of Papers for Eighth International Thermal Spraying Conference*, September 27 to October 1, 1976 (Miami Beach, FL, USA), p 381-384
2. Y. Shimatani and M. Endou, On the Structure, Hardness of Surfalloy Sprayed Layer, and Diffusion of Major Elements Between Sprayed Layer and Substrate, *J. Thermal Spraying Soc. Japan.*, 1967, **4**(2), p 11-18, (in Japanese)
3. M. Toyota, K. Usuki, S. Iwanaga, and K. Shyoji, The Influence of the Fusing Treatment on the Hardness and Microstructure of Sprayed and Fused "Surfalloy S-6M," *J. Thermal Spraying Soc. Japan.*, 1969 **6**(1), p 11-18, (in Japanese)
4. Y. Mima, M. Magome, H. Nakahira, and T. Morishita, On the Mechanical Properties of Spray Deposits Fused of self-fluxing Alloys, *J. Thermal Spraying Soc. Japan.*, 1976, **13**(1), p 22-28, (in Japanese)
5. W. Milewski and M. Sartowski, Some Properties of Coatings Plasma Sprayed from NiCrBSi Materials, *Preprints of Papers for 10th International Thermal Spraying Conference*, May 2-6, 1983 (Essen, Germany), p 8-11
6. O. Knotek, H. Reimann, and P. Lohang, On NiCrBSi Matrix-Carbide Reactions in Furnace Densified Wear Resistant Overlays, *Preprints for 10th International Thermal Spraying Conference*, May 2-6, 1983 (Essen, Germany), p 15-17
7. W.J. Lenling, M.F. Smith, and J.A. Henfling, Beneficial Effects of Austempering Post-Treatment on Tungsten Carbide Based Wear Coatings, *Proceedings of the 3rd National Thermal Spraying Conference*, May 20-25,1990 (Long Beach, CA, USA), p 227-232
8. S. Sampath, V. Anand, and S.F. Wayne, Microstructure and Properties of Plasma Sprayed Mo/NiCrBSi Coatings, *Proceedings of the 3rd National Thermal Spraying Conference*, May 20-25,1990 (Long Beach, CA, USA), p 755-760
9. K. Hidaka, K. Tanaka, S. Nishimura, and K. Kawarada, Hot Corrosion Resistance of a Chromium-Based Alloy Coating, *Proceedings for 14th International Thermal Spraying Conference*, May 22-26, 1995 (Kobe, Japan), p 609-614
10. H. Akebono, H. Nishimori, J. Komotori, and M. Shimizu, The Effect of Coating Thickness on Fatigue Properties of Ni-based Self-Fluxing Alloy Thermally Sprayed Steel with Long Period Fusing, *J. Thermal Spraying Soc. Japan.*, 1996, **33**(4), p 7-15, (in Japanese)
11. K. Kishitake, H. Era, F. Otsubo, and H. Ohhara, Structure of Ni-Based Self Fluxing Alloy Coating and Interface Reaction with Substrate, *J. Thermal Spraying Soc. Japan.*, 1989, **25**(4), p 1-8, (in Japanese)
12. F. Otsubo, K. Kishitake, and T. Terasaki, Residual Stress Distribution in Thermally Sprayed Self-Fluxing Alloy Coatings, *J. Thermal Spraying Soc. Japan.*, 2006, **43**(2), p 42-46, (in Japanese)
13. Y. Matsubara, Y. Sochi, M. Tanabe, and A. Takeya, Advanced Coatings on Furnace Wall Tubes, *Building on 100 Years of Success: Proceedings of the 2006 International Thermal Spray Conference*, B. R. Marple, M. M. Hyland, Y. C. Lau, R. S. Lima, and J. Voyer, Ed., May 15-18, 2006 (Seattle, WA, USA), ASM International, 2006
14. Y. Matsubara, K. Kohira, T. Uchibayasi, and K. Sakata, Diffusion Treatment of Thermal Sprayed Co-base Cr-W-B-Si Alloy Coating, *J. Thermal Spraying Soc. Japan.*, 1989, **25**(4), p 1-8, (in Japanese)
15. Y. Matsubara, K. Kohira, K. Sakata, and T. Uchubayashi, Microstructual Variation of Thermal Sprayed Co-Cr-W-B Alloy Coatings due to Diffusion Treatment, *Proceedings of Surface Engineering International Conference*, Oct 18-22, 1988 (Tokyo, Japan), Japan Thermal Spraying Society, p 53-62
16. J. Oh, J. Komotori, and M. Shimizu, Fatigue Strength and Fracture Mechanism of Thermally Sprayed Co-Based Self-Fluxing Alloy with Fusing Treatment, *J. Thermal Spraying Soc. Japan.*, 2000, **37**(4), p 166-174, (in Japanese)